

# Highly sensitive fluorescent sensor for mercury based on hyperbranched rolling circle amplification

Jinfeng Chen,<sup>ac</sup> Ping Tong,<sup>ab</sup> Yifen Lin,<sup>a</sup> Wei Lu,<sup>a</sup> Yu He,<sup>\*a</sup> Minghua Lu,<sup>b</sup> Lan Zhang<sup>\*ab</sup> and Guonan Chen<sup>a</sup>

Cite this: DOI: 10.1039/c4an01769b

Received 30th September 2014  
Accepted 16th November 2014

DOI: 10.1039/c4an01769b

www.rsc.org/analyst

A label-free hyperbranched rolling circle amplification (HRCA) based fluorescent sensor has been developed for Hg<sup>2+</sup> detection. The fluorescence intensity has a linear relationship with the concentration of the target in the range of 0.425 pmol L<sup>-1</sup> to 42.5 nmol L<sup>-1</sup>, and the detection limit is as low as 0.14 pmol L<sup>-1</sup> (S/N = 3). The proposed sensor had been applied to detect Hg<sup>2+</sup> in water samples with satisfying results.

## Introduction

Heavy metals show a great trend to form complexes, especially with ligands of biological matter containing nitrogen, sulfur, and oxygen. As a result, changes in the molecular structure of proteins, breaking of hydrogen bonds, or inhibition of enzymes can occur. These interactions, among others, may explain the toxicological and carcinogenic effects of heavy metals such as those affecting the central nervous system (Hg<sup>2+</sup>, Pb<sup>2+</sup>, As<sup>3+</sup>), the kidneys or liver (Cu<sup>2+</sup>, Cd<sup>2+</sup>, Hg<sup>2+</sup>, Pb<sup>2+</sup>), or skin, bones, or teeth (Ni<sup>2+</sup>, Cu<sup>2+</sup>, Cd<sup>2+</sup>, Cr<sup>3+</sup>).<sup>1–4</sup> So, heavy metal ions have received great attention recently.<sup>5–7</sup> The mercuric ion (Hg<sup>2+</sup>) is a highly toxic heavy metal which has been released frequently from industrial wastes and natural activities into the aquatic environment.<sup>8</sup> A number of severe health problems, such as brain damage, kidney failure, and cognitive and emotional disorders, can be caused by Hg<sup>2+</sup> contamination even at low concentrations,<sup>9,10</sup> so determination of Hg<sup>2+</sup> is highly important. Many traditional analytical approaches, such as atomic absorption or emission spectroscopy,<sup>11,12</sup> inductively coupled plasma-mass spectrometry<sup>13</sup> and selective cold vapor atomic fluorescence spectrometry,<sup>14</sup> have been frequently used to detect Hg<sup>2+</sup>. But these methods generally involve tedious sample preparation, and expensive and sophisticated instrumentation, which significantly limit their portability. It had been reported that Hg<sup>2+</sup> can specifically bind to thymine–thymine (T–T) base pairs in DNA duplexes.<sup>15</sup> The binding of mercury in T–Hg<sup>2+</sup>–T pairs is strong and highly selective; many sensors based on this base pair have already been developed.<sup>16–18</sup>

Lots of signal amplification strategies have been developed to achieve ultrasensitive detection.<sup>19</sup> Polymerase chain reaction (PCR) is the most conventional signal application for ultrasensitive assays. However, the PCR-based amplification strategy is time-consuming, sometimes nonspecific, and limited to a thermostable enzyme and a laboratory setting, and the heavy metal ions might affect the enzyme activity, so it is difficult to adapt PCR for the measurement of heavy metal ions.<sup>20–22</sup> Rolling circle amplification (RCA), an isothermal amplification technique, has attracted increasing attention in the development of biosensing systems due to its simplicity and high efficiency.<sup>23</sup> Based on the RCA reaction, hyperbranched rolling circle amplification (HRCA) has been developed,<sup>24</sup> which is an isothermal and exponential amplification through a turn-by-turn cascade of primer extension and strand displacement.<sup>25–27</sup> The products of HRCA consist of large amounts of single-stranded DNA (ss-DNA) and double-stranded DNA (ds-DNA) with various lengths. Many HRCA based biosensors have been developed for different targets, such as single nucleotide polymorphism,<sup>28</sup> RNA,<sup>29,30</sup> proteins,<sup>31,32</sup> and so on. But to the best of our knowledge, no studies about HRCA-based sensors for heavy metals have been reported, because it is considerably more difficult to combine the HRCA reaction with the a heavy metal assay.

In this study, a highly sensitive label-free HRCA based fluorescent sensor for Hg<sup>2+</sup> has been developed, which combines the advantage of efficient exponential amplification of HRCA and the stable biomimetic structure of T–Hg<sup>2+</sup>–T. Comparing our present work with other fluorescence, colorimetric and electrochemical methods for the detection of Hg<sup>2+</sup>, the detection limit of our strategy is lower than those of electrochemical methods and much better than those of other fluorescent and colorimetric sensors for Hg<sup>2+</sup>. For example, Qi *et al.*<sup>33</sup> developed a fluorescence sensing strategy for the detection of Hg<sup>2+</sup> and the detection limit was 0.2 nM. Guo *et al.*<sup>34</sup> recently reported a colorimetric sensing strategy employing silver nanoparticles

<sup>a</sup>Ministry of Education Key Laboratory of Analysis and Detection for Food Safety, Fujian Provincial Key Laboratory of Analysis and Detection for Food Safety, College of Chemistry, Fuzhou University, Fuzhou, Fujian 350108, China

<sup>b</sup>Testing Center, The Sport Science Research Center, Fuzhou University, Fuzhou, Fujian 350002, China

<sup>c</sup>Longyan Entry-Exit Inspection and Quarantine Bureau of P.R.C., Longyan, Fujian 364000, China

(AgNPs) to detect trace  $\text{Hg}^{2+}$  with a detection limit of 0.31 nM. Chen *et al.*<sup>35</sup> constructed an electrochemical monitoring strategy for  $\text{Hg}^{2+}$  with a detection limit of 0.02 nM. Based on the amplification of HRCA, this strategy pushed the detection limit down to 0.14 pM and the proposed sensor has also been applied to detect mercury in water samples.

## Experimental sections

### Materials and chemicals

DNA oligonucleotides were synthesized by Sangon Inc. (Shanghai, China). Their sequences are shown below:

Trigger: 5'-GTT TCG-3'

Primer 1: 5'-acGGc AAcca-3'

Primer 2: 5'-ggTCT cTTgT-3'

Padlock: 5'-P-TAC ÀcÀÀg ÀGÀc acGGc AAcca CGT-3'.

In the padlock probe, the region with the same sequence as the HRCA primer 1 is underlined and the binding region for the HRCA primer 2 is shown with a dotted line. An *Escherichia coli* (*E. coli*) DNA ligase set (including *Escherichia coli* DNA ligase, 10× *Escherichia coli* DNA ligase buffer, and 10× BSA (0.05%)) was obtained from Takara Biotechnology Co., Ltd. (Dalian, China). The deoxynucleotide solution mixture (dNTPs), Bst DNA polymerase large fragment, and their corresponding buffers were purchased from New England Biolabs (NEB). SYBR Green I was purchased from Xiamen Biovision Biotechnology Co. Ltd. (Xiamen, China). All other chemicals were of analytical reagent grade and obtained from Sigma Chemical Co., USA. Double distilled water (Milli-Q, Millipore, resistance 18.2 MΩ) was used throughout the experiments. DNA buffer solutions were prepared by dissolving DNA in 50 mmol L<sup>-1</sup> Tris-HCl (pH 7.4).

### HRCA reaction and $\text{Hg}^{2+}$ detection

Hybridization of the trigger probes with the padlock probes was carried out in a system containing 50 nmol L<sup>-1</sup> padlock probe, 50 nmol L<sup>-1</sup> trigger probe and different concentrations of  $\text{Hg}^{2+}$ . The above solution was incubated at 37 °C for 60 min under shaking. The ligation reaction was performed in ligation buffer solution containing 6 U *E. coli* DNA ligase, 0.05% BSA and 0.167 mmol L<sup>-1</sup> nicotinamide adenosine dinucleotides (NAD), which was incubated at 37 °C for 60 min. Then, the HRCA reaction was carried out at 63 °C for 60 min in a solution including 50 nmol L<sup>-1</sup> primer 1, 50 nmol L<sup>-1</sup> primer 2, 9.6 U Bst DNA polymerase and 0.6 mmol L<sup>-1</sup> dNTP. Finally, the reaction was terminated by heating at 95 °C for 5 min.

### Fluorescence detection

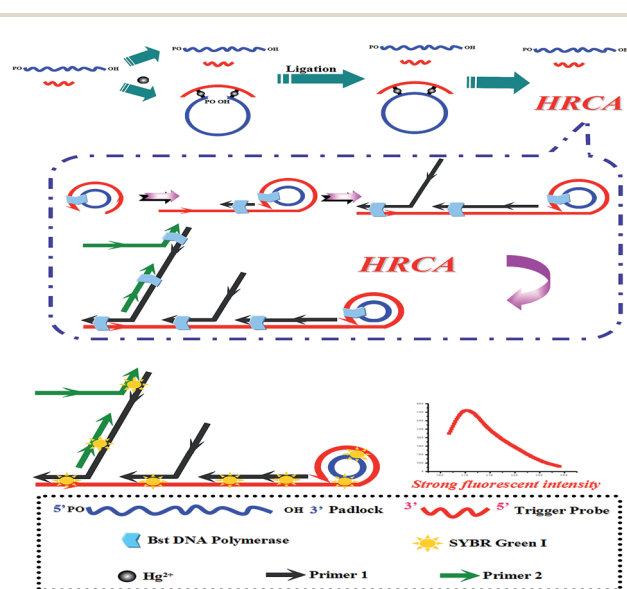
The product obtained using the above HRCA products and 4 μL SYBR Green I were mixed and incubated at room temperature for 10 min. The fluorescence measurements were performed at room temperature on a Varian Cary Eclipse Fluorescence Spectrophotometer except specific indication. The emission spectra were collected from 500 to 600 nm with an excitation wavelength of 488 nm. Both excitation and emission slit widths were set to 10.0 nm. All measurements were repeated three

times and the average value of fluorescence intensity at 520 nm was used for quantitative analysis.

## Results and discussion

The principle of the biosensor T-T (thymine–thymine) mispairs in DNA duplexes is to capture  $\text{Hg}^{2+}$  ions and form stable neutral base pairs [T– $\text{Hg}^{2+}$ –T]. The formation of such complexes results in stabilization of the duplex depending on the number of consecutive [T– $\text{Hg}^{2+}$ –T] pairs.<sup>36</sup> The principle of the proposed biosensor is schematically shown in Scheme 1. The trigger probe is designed to complement the two termini of the circular padlock probe but with two T-T mismatches. This mismatch cannot be hybridized and extended in the absence of  $\text{Hg}^{2+}$ . In the presence of  $\text{Hg}^{2+}$ , the two termini of the padlock probe are perfectly hybridized with the complementary trigger probe through the stable T– $\text{Hg}^{2+}$ –T biomimetic structure, thus the 5' and 3' ends of the padlock probe are brought together and a circular padlock probe is generated in the presence of *E. coli* DNA ligase. Subsequently, the HRCA reaction is initiated. Briefly, the trigger probe is extended isothermally at its 3' end by Bst DNA polymerase to generate multimeric single-stranded DNA (ss-DNA), which serves as the template for the primer 1 binding. Primer 1 is further extended by Bst DNA polymerase to displace the downstream growing DNA strand. This displacing strand again contains multiple binding sites for primer 2 hybridization. As a result, large amounts of different length ss-DNA and double-stranded DNA (ds-DNA) can be produced. Since ds-DNA can combine with SYBR Green I to produce a strong fluorescent signal, the signal intensity might work as a quantitative basis for  $\text{Hg}^{2+}$  detection, based on which, a sensitive fluorescent  $\text{Hg}^{2+}$  sensor can be developed.

A simple experiment was performed to verify the feasibility of the proposed method. As shown in Fig. 1, in the absence of target ( $\text{Hg}^{2+}$ ), the fluorescence intensity is weak (curve a),



Scheme 1 The mechanism of the biosensor for mercuric ions ( $\text{Hg}^{2+}$ ) based on HRCA.

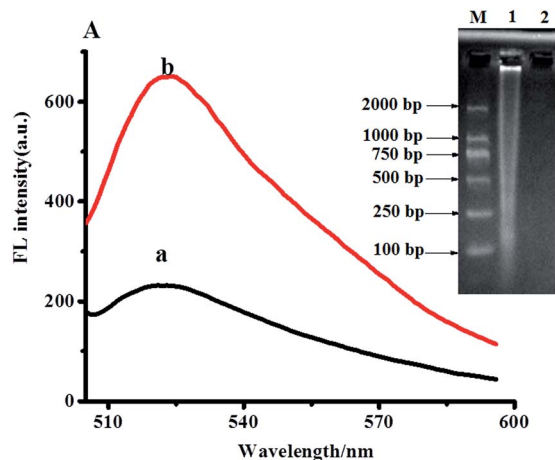


Fig. 1 Fluorescence spectra of the system in the absence (curve a) and presence (curve b) of  $\text{Hg}^{2+}$  ( $4.25 \times 10^{-8} \text{ mol L}^{-1}$ ) based on HRCA. Inset: HRCA products are electrophoresed in a 2% agarose gel. The DNA ladder is indicated in lane M. Lanes 1 and 2 represent the HRCA products in the presence and absence of  $\text{Hg}^{2+}$  ( $4.25 \times 10^{-8} \text{ mol L}^{-1}$ ), respectively.

indicating that HRCA does not occur and little ds-DNA has been formed. Once the T-Hg<sup>2+</sup>-T biomimetic structure is formed, an obvious fluorescence enhancement was detected (curve b), which indicates that the HRCA reaction was initiated and large amounts of ds-DNA were produced. To further verify the validity of the proposed method, the HRCA products were analyzed with gel electrophoresis experiments. As shown in the inset of Fig. 1, no bands in the absence of  $\text{Hg}^{2+}$  are observed (lane 2) since no HRCA products occur, while in the presence of  $\text{Hg}^{2+}$ , an obvious smear appears in lane 1 because the molecular weight of the HRCA products is an approximate range but not an exact numerical value. These results indicate that various lengths of DNA strands are generated through HRCA, which could be used to detect  $\text{Hg}^{2+}$  with high sensitivity.

### Optimization of the reaction conditions

To achieve a better sensing performance, the concentrations of dNTP and Bst DNA polymerase have been optimized. As shown in Fig. 2(A), with increasing the dNTP concentration, the fluorescence intensity is gradually enhanced, and finally reaches a constant value after  $0.6 \text{ mmol L}^{-1}$ . Therefore,  $0.6 \text{ mmol L}^{-1}$  has been chosen as the optimum concentration of dNTP in the following experiments. Similarly, the concentration of Bst DNA polymerase was also investigated. As shown in Fig. 2(B), the fluorescence intensity firstly increased and then reached a stabilized plateau when the concentration of Bst DNA polymerase was higher than 9.6 U. Thus, 9.6 U was chosen as the optimum condition in the following studies.

It is well known that mercury above a certain concentration can cause a decrease in enzyme activity or even completely kill the activity of enzymes such as papain and invertase. In spite of the efforts reported so far, the effect of  $\text{Hg}^{2+}$  on the activities of *E. coli* ligase and Bst polymerase has not been reported. Therefore, this study has also been performed, as shown in

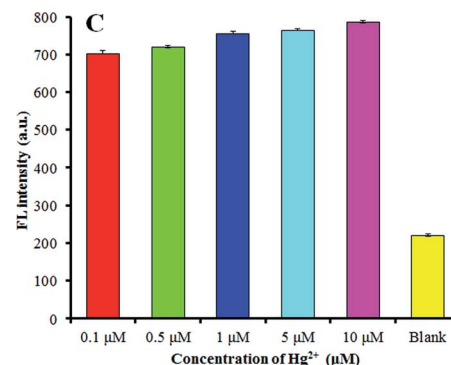
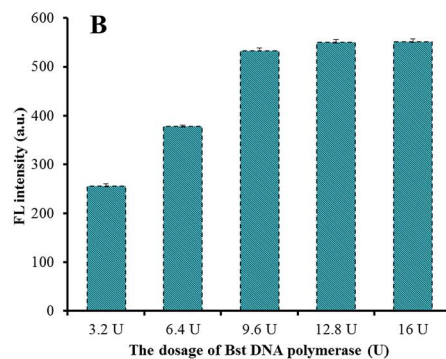
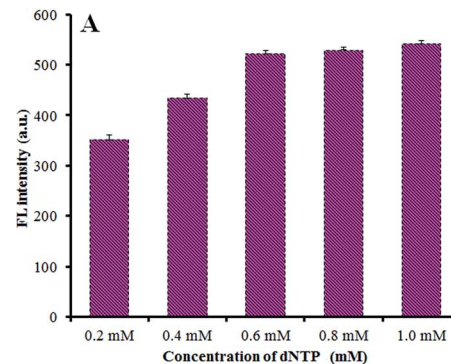


Fig. 2 (A) Effect of dNTP concentration on the fluorescence intensity of the system. (B) Effect of the dosage of Bst DNA polymerase on the fluorescence intensity of the system ( $[\text{Hg}^{2+}] = 4.25 \times 10^{-9} \text{ mol L}^{-1}$ ). (C) Effect of  $\text{Hg}^{2+}$  concentration on the fluorescence intensity of the system.

Fig. 2(C), with an increase in  $\text{Hg}^{2+}$  concentration, the fluorescence intensity was gradually enhanced. When the concentration of  $\text{Hg}^{2+}$  reached up to  $10 \mu\text{mol L}^{-1}$ , the fluorescence intensity was still not affected. This means that a  $\text{Hg}^{2+}$  concentration below  $10 \mu\text{mol L}^{-1}$  should not decrease the enzyme activity.

### Quantitative analysis of $\text{Hg}^{2+}$

Different concentrations of  $\text{Hg}^{2+}$  were added into the solution and the corresponding fluorescence intensity was detected. Fig. 3(A) shows the fluorescence spectra at different  $\text{Hg}^{2+}$

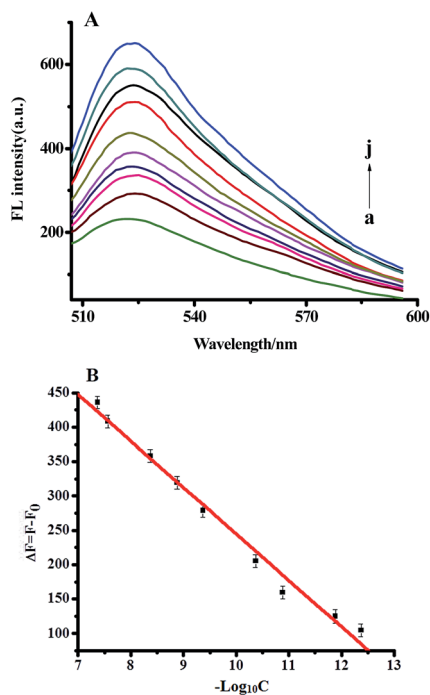


Fig. 3 (A) Fluorescence spectra in the presence of different concentrations of  $\text{Hg}^{2+}$ . (a–j)  $0$ ,  $4.25 \times 10^{-13}$ ,  $1.31 \times 10^{-12}$ ,  $1.31 \times 10^{-11}$ ,  $4.25 \times 10^{-11}$ ,  $4.25 \times 10^{-10}$ ,  $1.31 \times 10^{-9}$ ,  $4.25 \times 10^{-9}$ ,  $2.73 \times 10^{-8}$ , and  $4.25 \times 10^{-8}$  mol  $\text{L}^{-1}$ . (B) Plot of enhanced fluorescence intensity versus logarithm of  $\text{Hg}^{2+}$  concentration. The error bars show the standard deviation of three replicate determinations.

concentrations; the introduction of higher  $\text{Hg}^{2+}$  concentrations results in higher fluorescence intensities. Fig. 3(B) shows the linear relationship between the enhanced fluorescence intensity of the system and the  $\text{Hg}^{2+}$  concentration. The enhanced fluorescence intensity has a direct relationship with the logarithm of the  $\text{Hg}^{2+}$  concentration in the range of  $4.25 \times 10^{-13}$  to  $4.25 \times 10^{-8}$  mol  $\text{L}^{-1}$ . The resulting regression equation is:

$$\Delta F = 67.65 \log_{10} C + 920.6, R = 0.9934$$

where  $C$  is the concentration of  $\text{Hg}^{2+}$ , and  $\Delta F$  is the change in fluorescence after the addition of targets, which was calculated by using the formula:  $\Delta F = F - F_0$ .  $F$  and  $F_0$  are fluorescence intensities at 520 nm in the presence and absence of  $\text{Hg}^{2+}$ .  $R$  is the regression coefficient of the equation. Based on this method, the detection limit for  $\text{Hg}^{2+}$  was estimated as  $1.4 \times 10^{-13}$  mol  $\text{L}^{-1}$  (defined as  $S/N = 3$ ).

Six replicate experiments were performed at the  $\text{Hg}^{2+}$  concentration of  $50 \text{ pmol L}^{-1}$ , and the relative standard deviation (RSD) was 5.28%. This means the proposed method shows good reproducibility. In addition, after being stored in a refrigerator at  $4 \text{ }^\circ\text{C}$  for four weeks, the DNA buffer was used again to detect  $\text{Hg}^{2+}$ , the detected signals showed no significant change compared with that using the freshly prepared solution. These results suggest that this proposed sensor has a good stability.

### Specificity and application of sensor

The selectivity of the sensor was determined by challenging it with various competing metal ions such as  $\text{Cu}^{2+}$ ,  $\text{Cd}^{2+}$ ,  $\text{Pb}^{2+}$ ,  $\text{Ni}^{2+}$ ,  $\text{Fe}^{2+}$ ,  $\text{Li}^+$ ,  $\text{Mn}^{2+}$ , and  $\text{Ag}^+$  ( $1 \text{ } \mu\text{mol L}^{-1}$ ). As shown in Fig. 4,  $\text{Hg}^{2+}$  ( $4.27 \times 10^{-11}$  mol  $\text{L}^{-1}$ ) showed the highest signal and the responses from the interferences are very low. It was obvious that the specific recognition of the T-T mismatch bases by  $\text{Hg}^{2+}$  ions endowed the sensor with high selectivity.

To investigate the application of the proposed sensor in real samples, the  $\text{Hg}^{2+}$  concentration was studied in three water samples (lake, river and tap water). The lake water was from Fuzhou University and the river water was from the Minjiang River in Fuzhou. As shown in Table 1, the concentrations of  $\text{Hg}^{2+}$  in the water samples were  $0$ ,  $1.81 \times 10^{-13}$  mol  $\text{L}^{-1}$ , and  $1.36 \times 10^{-13}$  mol  $\text{L}^{-1}$ . Furthermore, to evaluate the reliability of our sensor system, the recovery was investigated by adding two different amounts of  $\text{Hg}^{2+}$  into all three samples, and the recovery was calculated as 96.6–102%. Therefore, the developed sensor could be preliminarily applied for the determination of  $\text{Hg}^{2+}$  in water samples.

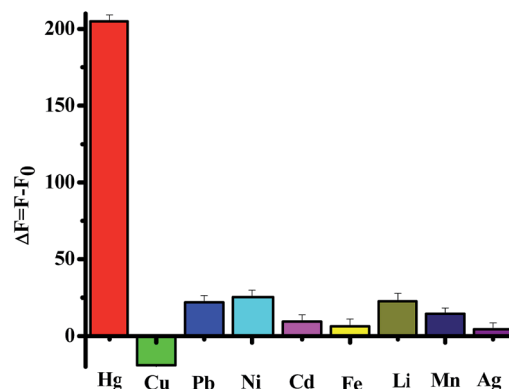


Fig. 4 Change in fluorescence intensity of the proposed sensor with different interferences. The concentration of  $\text{Hg}^{2+}$  was  $4.27 \times 10^{-11}$  mol  $\text{L}^{-1}$ , while the concentration of the other interferences was  $1 \times 10^{-6}$  mol  $\text{L}^{-1}$ .

Table 1 Recoveries of the proposed method for determination of  $\text{Hg}^{2+}$  in different water samples<sup>a</sup>

Sample	Detected (mol $\text{L}^{-1}$ )	Added (mol $\text{L}^{-1}$ )	Found (mol $\text{L}^{-1}$ )	Recovery (%)
Tap water	—	$1.50 \times 10^{-12}$ $3.00 \times 10^{-12}$	$1.53 \times 10^{-12}$ $2.88 \times 10^{-12}$	102 96.0
River water	$1.81 \times 10^{-13}$	$1.50 \times 10^{-12}$ $3.00 \times 10^{-12}$	$1.63 \times 10^{-12}$ $2.93 \times 10^{-12}$	96.6 97.7
Lake water	$1.36 \times 10^{-13}$	$1.50 \times 10^{-12}$ $3.00 \times 10^{-12}$	$1.62 \times 10^{-12}$ $2.98 \times 10^{-12}$	98.9 99.3

<sup>a</sup> “—” means not detected.

## 1 Conclusion

5 In summary, a new selective and sensitive fluorescent sensing system for Hg<sup>2+</sup> has been developed by merging the structure of T-Hg<sup>2+</sup>-T with the isothermal and exponential amplification of HRCA technology. This homogeneous assay system not only eliminates thermal cycling but also achieves improved assay characteristics (e.g., wide linear response range, low detection limit and high specificity). Moreover, the proposed method has enormous potential for the application of Hg<sup>2+</sup> monitoring in the environment, and water and food samples.

## 15 Acknowledgements

15 This project was financially supported by the National Nature Sciences Foundation of China (21275029), the National Basic Research Program of China (no. 2010CB732403), the “12th Five-Year National Science and Technology Support Program” (2012BAD29B06), the Natural Science Foundation of Fujian Province (2010J05021), the Program for Changjiang Scholars and Innovative Research Team in University (no. IRT1116) and the Educational Research Project in Fujian Province (JA14055).

## 25 Notes and references

- 1 J. W. Hamilton, R. C. Kaltreider, O. V. Bajenova, M. A. Ilnat, J. McCaffrey, B. W. Turpie, E. E. Rowell, J. Oh, M. J. Nemeth, C. A. Pesce and J. R. Lariviere, *Environ. Health Perspect.*, 1998, **106**, 1005.
- 2 B. L. Vallee and D. D. Ulmer, *Annu. Rev. Biochem.*, 1972, **41**, 91.
- 3 T. Partanen, P. Heikkila, S. Hernberg, T. Kauppinen, G. Moneta and A. Ojajarvi, *Scand. J. Work, Environ. Health*, 1991, **17**, 231.
- 4 H. B. Teh, H. Li and S. F. Y. Li, *Analyst*, 2014, **139**, 5170.
- 5 E. L. Que, D. W. Domaille and C. J. Chang, *Chem. Rev.*, 2008, **108**, 1517.
- 6 M. Benounis, N. Jaffrezic-Renault, H. Halouani, R. Lamartine and I. Dumazet-Bonnamour, *Mater. Sci. Eng., C*, 2006, **26**, 364–368.
- 7 R. McRae, P. Bagchi, S. Sumalekshmy and C. J. Fahrni, *Chem. Rev.*, 2009, **109**, 4780.
- 8 P. R. Srinivas, S. Srivastava, S. Hanash and G. L. J. Wright, *Clin. Chem.*, 2001, **47**, 1901.
- 9 S. K. Arya and S. Bhansali, *Chem. Rev.*, 2011, **111**, 6783.
- 10 M. Ferrari, *Nat. Rev. Cancer*, 2005, **5**, 161.
- 11 J. B. Willis, *Anal. Chem.*, 1962, **34**, 615.
- 12 F. X. Han, W. D. Patterson, Y. Xia, B. B. M. Sridhar and Y. Su, *Water, Air, Soil Pollut.*, 2006, **170**, 161.
- 13 D. S. Bushee, *Analyst*, 1988, **113**, 1167.

- 14 N. Pourreza and K. Ghanemi, *J. Hazard. Mater.*, 2009, **161**, 982.
- 15 A. Ono and H. Togashi, *Angew. Chem., Int. Ed.*, 2004, **43**, 4300–4302.
- 16 S. Tang, P. Tong, W. Lu, J. Chen, Z. Yan and L. Zhang, *Biosens. Bioelectron.*, 2014, **59**, 1–5.
- 17 M. Zhang, H. Le, X. Jiang and B. Ye, *Chem. Commun.*, 2013, **49**, 2133.
- 18 G. Zhu, Y. Li and C. Y. Zhang, *Chem. Commun.*, 2014, **50**, 572–574.
- 19 Y. F. Wu, W. Wei and S. Q. Liu, *Acc. Chem. Res.*, 2012, **45**, 1441.
- 20 B. Zhang, B. Liu, D. Tang, R. Niessner, G. Chen and D. Knopp, *Anal. Chem.*, 2012, **84**, 5392.
- 21 J. Huang, Y. Chen, L. Yang, Z. Zhu, G. Zhu, X. Yang, K. Wang and W. Tan, *Biosens. Bioelectron.*, 2011, **28**, 450.
- 22 L. Zhang, S. Guo, S. Dong and E. Wang, *Anal. Chem.*, 2012, **84**, 3568.
- 23 Z. Zhang and C. Zhang, *Anal. Chem.*, 2012, **84**, 1623.
- 24 P. M. Lizardi, X. H. Huang, Z. G. Zhu, P. Bray-Ward, D. C. Thomas and D. C. Ward, *Nat. Genet.*, 1998, **19**, 225.
- 25 D. Y. Zhang, W. Zhang, X. Li and K. Konomi, *Gene*, 2001, **274**, 209.
- 26 Y. Q. Cheng, X. Zhang, Z. Li, X. Jiao, Y. Wang and Y. Zhang, *Angew. Chem., Int. Ed.*, 2009, **121**, 3318.
- 27 L. R. Zhang, G. Zhu and C. Y. Zhang, *Anal. Chem.*, 2014, **86**, 6703–6709.
- 28 S. Kaocharoen, B. Wang, K. M. Tsui, L. Trilles, F. Kong and W. Meyer, *Electrophoresis*, 2008, **29**, 3183.
- 29 B. Wang, S. J. Potter, Y. Lin, A. L. Cunningham, D. E. Dwyer, Y. Su, X. Ma, Y. Hou and N. K. Saksena, *J. Clin. Microbiol.*, 2005, **43**, 2339.
- 30 Y. Q. Cheng, X. Zhang, Z. Li, X. Jiao and Y. Wang, *Angew. Chem., Int. Ed.*, 2009, **48**, 3268.
- 31 Q. Wang, H. Zheng, X. Gao, Z. Lin and G. Chen, *Chem. Commun.*, 2013, **49**, 11418.
- 32 X. Zhu, H. Xu, H. Zheng, G. Yang, Z. Lin, B. Qiu, L. Guo, Y. Chi and G. Chen, *Chem. Commun.*, 2013, **49**, 10115.
- 33 L. Qi, Y. Zhao, H. Yuan, K. Bai, Y. Zhao, F. Chen, Y. Dong and Y. Wu, *Analyst*, 2012, **137**, 2799.
- 34 Z. Guo, G. Chen, G. Zeng, Z. Li, A. Chen, M. Yan, L. Liua and D. Huang, *RSC Adv.*, 2014, **4**, 59275.
- 35 J. Chen, J. Tang, J. Zhou, L. Zhang, G. Chen and D. Tang, *Anal. Chim. Acta*, 2014, **810**, 10–16.
- 36 Y. Miyake, H. Togashi, M. Tashiro, H. Yamaguchi, S. Oda, M. Kudo, Y. Tanaka, Y. Kondo, R. Sawa, T. Fujimoto, T. Machinami and A. Ono, *J. Am. Chem. Soc.*, 2006, **128**, 2172.